Velocity versus momentum relaxation of electrons in a magnetic field

1999 J. Phys.: Condens. Matter 11 4009

(http://iopscience.iop.org/0953-8984/11/20/307)

J. Phys.: Condens. Matter **11** (1999) 4009–4019. Printed in the UK PII: S0953-8984(99)00249-0

Velocity versus momentum relaxation of electrons in a magnetic field

A Svizhenko† S Bandyopadhyay†§ and M A Stroscio‡

† Department of Electrical Engineering, University of Nebraska, Lincoln, NE 68588, USA
‡ US Army Research Office, PO Box 12211, Research Triangle Park, NC 27709, USA

E-mail: bandy@engrs.unl.edu

Received 21 December 1998, in final form 4 March 1999

Abstract. In a parabolic band, the momentum and velocity relaxation rates of electrons (associated with scattering) are identical. However, if a magnetic field is present, they are fundamentally different quantities that can have *opposite* signs over quite wide ranges of the electron's kinetic energy. Consequently, it is possible that electrons will *lose* momentum during a scattering event and yet *gain* velocity. In narrow InAs quantum wires subjected to a high magnetic field, we show that this can cause the ensemble average momentum and velocity relaxation rates to have opposite signs in realistic situations.

1. Introduction

The difference between the 'dynamical momentum' and 'kinematic momentum' of an electron in a magnetic field is well known in the context of both classical [1] and quantum mechanics [2]. In a crystal, the dynamical momentum is the crystal momentum $\hbar\vec{k}$ (where $\vec{k}$ is the electron's wavevector) and the kinematic momentum is $m^*\vec{v}$ (where $\vec{v}$ is the electron's velocity and m^* the effective mass which is constant if the conduction band is parabolic). The two are related by $\hbar\vec{k} = m^*\vec{v} + q\vec{A}$ where q is the particle charge and $\vec{A}$ is the magnetic vector potential. This difference between $\hbar\vec{k}$ and $m^*\vec{v}$ automatically causes a difference between the momentum and velocity relaxation rates whenever a magnetic field is present.

2. Velocity and momentum relaxation of carriers in a magnetic field

We will study the above difference in a quantum wire which has only one free direction for particle transport. An external magnetic field is applied perpendicular to the wire axis and an electric field is oriented along the axis to induce carrier transport. The momentum and velocity relaxation rates, τ_m^{-1} and τ_v^{-1}, associated with phonon scattering, are calculated from the usual prescription of weighting the scattering rate $S(E_\nu, E'_{\nu'} \pm \gamma, \pm\omega_\gamma)$ by the relative momentum or velocity change, and then integrating over all possible final electron states and phonon wavevectors [3]:

$$\frac{1}{\tau_m(E_\nu)} = \frac{2L}{\pi}\sum_n \int_0^\infty \int_0^{\gamma_{max}} D(E'_{\nu'})\,\mathrm{d}E'_{\nu'}\,\mathrm{d}\gamma\; S(E_\nu, E'_{\nu'}, \pm\omega_{n,\gamma})(1 - f(E'_{\nu'}))\frac{(k-k')}{k} \tag{1}$$

§ Author to whom any correspondence should be addressed.

0953-8984/99/204009+11$19.50

$$\frac{1}{\tau_\nu(E_\nu)} = \frac{2L}{\pi}\sum_n \int_0^\infty \int_0^{\gamma_{max}} D(E'_{\nu'})\,\mathrm{d}E'_{\nu'}\,\mathrm{d}\gamma\; S(E_\nu, E'_{\nu'}, \pm\omega_{n,\gamma}) \times (1 - f(E'_{\nu'}))\frac{(v_\nu(k) - v'_{\nu'}(k'))}{v_\nu(k)} \tag{2}$$

where k is the electron's initial wavevector in the unconfined direction, $D(E'_{\nu'})$ is the density of final states, $f(E'_{\nu'})$ is the occupation probability of the electron's final state (after scattering) which is negligible compared to unity for a non-degenerate electron gas, E_ν is the electron's initial energy in the νth magnetoelectric transverse subband, $v_\nu(k)$ $(=(1/\hbar)(\partial E_\nu/\partial k))$ is the electron's initial velocity in that subband [6], $v'_{\nu'}(k')$ is the final velocity, γ is the wavevector of the phonon (of energy $\hbar\omega_{n,\gamma}$ belonging to the nth phonon branch) which is involved in the scattering and S is the scattering rate. The primed and unprimed quantities pertain to final and initial states of the electron respectively. Physically, the two quantities in equations (1) and (2) describe the rate at which momentum and velocity gained from a driving electric and/or magnetic field is lost to the lattice through phonon-mediated collisions. Thus, they are the rates that will enter a momentum or velocity balance equation.

A magnetic field affects the relaxation rates by altering $D(E'_{\nu'})$, S and, most importantly, $v_\nu(k)$ and $v'_{\nu'}(k')$. Note that the definition of velocity $v_\nu(k)$ $(v_\nu(k) = (1/\hbar)(\partial E/\partial k)$ [6]) is gauge independent and denotes a physical observable. The momentum $\hbar k$ also has a physical meaning since it is the quantity conserved in a scattering event with or without a magnetic field [4]. Thus, the quantities in equations (1) and (2) are physically meaningful.

In all our calculations, we rigorously account for both electron and phonon confinement. The magnetoelectrically confined electron states and their energy dispersion relations are found by solving the Schrödinger equation in a quantum wire subjected to a magnetic field [5] and the phonon normal modes as well as their dispersion relations are found by solving the elasticity equation numerically [8, 9]. In equations (1) and (2), the summation over the index n represents summation over confined phonon modes or branches. The calculations of the dispersion relations E_ν versus k for magnetoelectric subbands, the velocity $v_\nu(k)$, the electron wavefunctions in a magnetic field etc, have been described by us previously [5, 8, 9, 13] and will not be repeated here.

In the absence of a magnetic field ($\vec{A} = 0$), electron velocity in a parabolic band is always proportional to the momentum. Consequently (see equations (1) and (2)), the velocity and momentum relaxation rates are identical. However, when a magnetic field is present, the energy dispersion relations become immediately non-parabolic (see figure 2 later) with the result that the two rates are no longer equal. This, by itself, is not surprising, but what *is* counter-intuitive is that the two rates can even have opposite signs. It is this feature that we address and elucidate in this paper.

2.1. The origin of opposite signs: confined acoustic phonon scattering

In figure 1, we show the velocity-versus-wavevector relation for the three lowest magnetoelectric subbands in an intrinsic free-standing InAs quantum wire of rectangular cross section subjected to a magnetic flux density of 25 T [7]. These curves were calculated according to the prescription of reference [5]. Since they are not linear, velocity is *not* proportional to crystal momentum $\hbar k$ and hence τ_m^{-1} and τ_v^{-1} are distinct. Only at large wavevectors (when $\hbar k \gg q\vec{A}$) does the relationship begin to assume linearity. This figure also schematically depicts transitions that involve loss of momentum but gain of velocity (A–D), loss of momentum but no change in velocity (A–B) and gain of velocity but no change in momentum (A–C). In such transitions, clearly, $\tau_m^{-1} \neq \tau_v^{-1}$ and, in the first example (A–D), they even have opposite signs.

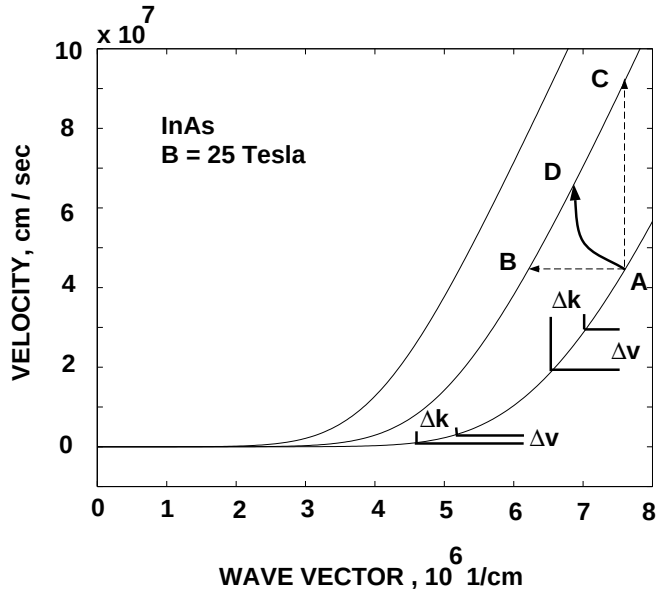

Figure 1. The solid curves represent the velocity-versus-wavevector relation for the first three subbands in an InAs quantum wire with rectangular cross section of 500 Å × 40 Å subjected to a magnetic field of 25 T. The conduction band is assumed to be parabolic. The broken line is the velocity–wavevector relation when no magnetic field is present (it is the same for all subbands). Shown are three transitions that result in no velocity relaxation but momentum relaxation (A–B), no momentum relaxation but velocity relaxation (A–C) and opposite signs of momentum and velocity relaxation (A–D). This figure also shows that the velocity change Δv for a given wavevector change Δk is much larger at large wavevectors than at small wavevectors. Consequently, a forward-scattering event and a backward-scattering event (with the same initial wavevector) which cause the same amount of momentum relaxation, result in unequal amounts of velocity relaxation. The forward-scattering event takes an electron to larger wavevectors and therefore is more efficient in relaxing velocity than the backscattering event which takes an electron to smaller wavevectors.

In figure 2, we show the energy-versus-wavevector (E_v–k) dispersion relations for the magnetoelectric subbands in a free-standing InAs wire of width 500 Å and thickness 40 Å. The magnetic flux density is 25 T. The flat regions of the subbands correspond to closed Landau orbits which have no resultant translational velocity (and hence have zero slope). A 'horizontal' transition of the type marked '1' will result in a non-zero momentum relaxation rate τ_m^{-1}, but no velocity relaxation and hence no τ_v^{-1}. This transition corresponds to scattering between two Landau orbits centred at two different locations. These are highly probable transitions since the scattering rate is proportional to the density of final states which is very large at the subband bottoms. One would assume that because of these transitions, the momentum relaxation rate should exceed the velocity relaxation rate and indeed it does when such *elastic* transitions are dominant. However, in this paper, we are considering *confined* phonon scatterings and most of them are inelastic (very few confined acoustic phonon branches can produce zero-energy phonons [9]). Nonetheless, it turns out that in the case of interactions with acoustic phonons (which still have relatively small energy), the transitions are quasi-elastic and almost 'horizontal' (of the type marked '3' in figure 2). Consequently, the momentum relaxation rate generally does exceed the velocity relaxation rate ($\tau_v^{-1} < \tau_m^{-1}$) for acoustic phonon interactions.

In figures 3(a) and 3(b), we show the velocity and momentum relaxation rates associated with non-polar acoustic (deformation potential) and polar acoustic (piezoelectric) phonon

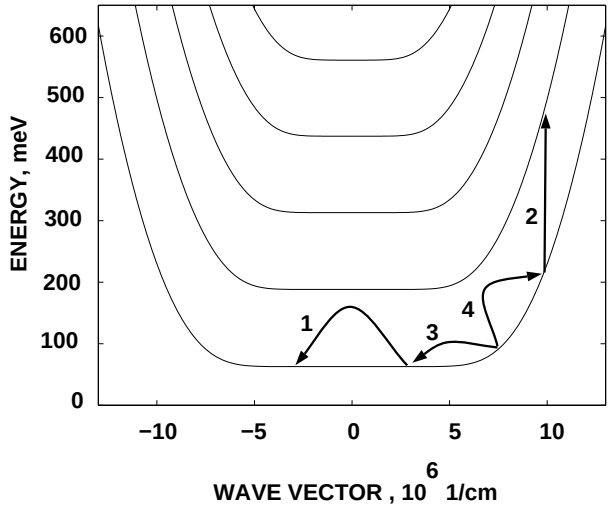

Figure 2. The energy–wavevector relation for magnetoelectric subbands in the InAs quantum wire in a magnetic flux density of 25 T. The transition '1' is a'horizontal' elastic backward intra-subband scattering which causes momentum relaxation but no velocity relaxation. Transition '2' is a 'vertical' inelastic inter-subband scattering with no change in momentum but a finite change in velocity. Transition '3' is a backward intra-subband emission with positive momentum and velocity relaxation rates and transition '4' is intra-subband absorption with a negative momentum and velocity relaxation rates.

scattering as functions of an electron's initial kinetic energy. The phonons are assumed to be in thermodynamic equilibrium, so their distribution is governed by Bose–Einstein statistics. The electron is always initially in the lowest subband. The peaks in the scattering rates arise from the van Hove singularities in the joint electron–phonon density of states [5, 8, 9, 13]. In the preceding paragraph we explained why $\tau_v^{-1} < \tau_m^{-1}$ for acoustic phonon interactions, but now we will explain why the two rates can even have *opposite* signs at energies well below the second subband bottom. At these low energies, electron interactions are mostly intra-subband scattering within the lowest magnetoelectric subband since the higher subbands are not accessible in energy (except by absorbing highly energetic phonons which are scarce because their population is governed by Bose–Einstein statistics). The two dominant intra-subband acoustic phonon scattering mechanisms in this case are *backward* emission and *forward* absorption. Backward scatterings are those in which an electron's forward momentum decreases ($k' < k$) whereas in forward scattering it increases ($k' > k$). Consequently, backscattering results in a positive momentum relaxation rate and forward scattering in a negative momentum relaxation rate. In a magnetic field, intra-subband backscattering events *which change the sign of an electron's momentum* are known to be strongly suppressed [10], but those which merely decrease the electron's momentum without changing its sign are not suppressed (the inset of figure 3(b) distinguishes between these two types of intra-subband backscattering; type '1' and type '2', respectively). In the case of deformation potential scattering, backward emission (of the second type) is quite frequent and dominates over forward absorption. Consequently, the overall momentum relaxation rate is *positive*. Backward emission of the second type also occurs in the transitions marked '3' in figure 2. Although they cause significant momentum relaxation, it should be obvious from figure 2 that they cause negligible velocity relaxation. On the other hand, forward absorption (the transition marked '4' in figure 2) causes much larger velocity relaxation for the same change in momentum. This

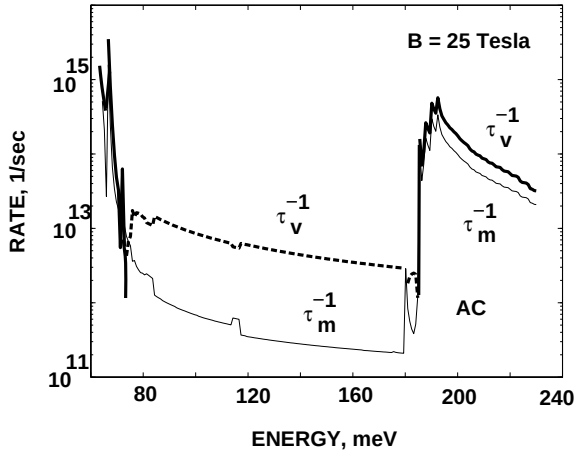

Figure 3. Velocity and momentum relaxation rates for acoustic phonon scattering in a magnetic flux density of 25 T and at a temperature $T = 77$ K. The rates are plotted versus initial electron kinetic energy which is measured from the bulk conduction band edge. Thin curves show the momentum relaxation rate and thick curves the velocity relaxation rate. The dashed curves indicate negative sign: (a) deformation potential scattering (AC); (b) piezoelectric scattering (PZ). The inset in (b) shows two different types of backward emission: (1) changes the sign of the electron's momentum and (2) does not change the sign although the momentum decreases. The third transition shows a backward absorption that changes the sign of the momentum.

fact becomes even clearer upon examining figure 1 which shows the relation between velocity and wavevector. Note that the curves in figure 1 are *superlinear*, so the velocity change Δv for a given wavevector change Δk is much smaller at small wavevectors than at large wavevectors (the Δv associated with two equal increments in k are shown in figure 1). As a consequence of this feature, forward absorption, even though rarer than backward emission of type 2, results in a much larger Δv and hence makes a larger contribution to the velocity relaxation than backward emission. Since the velocity relaxation rate associated with forward-scattering processes is negative, the overall velocity relaxation rate, unlike the momentum relaxation rate, is negative. All of this explains why τ_v^{-1} can be negative and τ_m^{-1} positive at low energies.

2.2. Confined longitudinal and surface optical phonon scattering

In figure 4(a) we show the momentum and velocity relaxation rates associated with longitudinal optical phonon scattering. For InAs, we assumed the following parameters [11, 12]: the longitudinal polar optical phonon (POP) energy $\hbar\omega_L = 30.2$ meV, the low-frequency relative permittivity $\epsilon_0 = 15.5$, the high-frequency relative permittivity $\epsilon_\infty = 12.3$. There are four distinct peaks in figure 4(a) corresponding to intra-subband POP absorption (at the first subband bottom), intra-subband POP emission (30.2 meV above the first subband bottom), inter-subband POP absorption (30.2 meV below the second subband bottom) and inter-subband POP emission (30.2 meV above the second subband bottom).

First, let us consider low energies below the second peak, i.e. below the polar optical phonon energy in InAs, so that all emission processes are blocked by energy conservation.

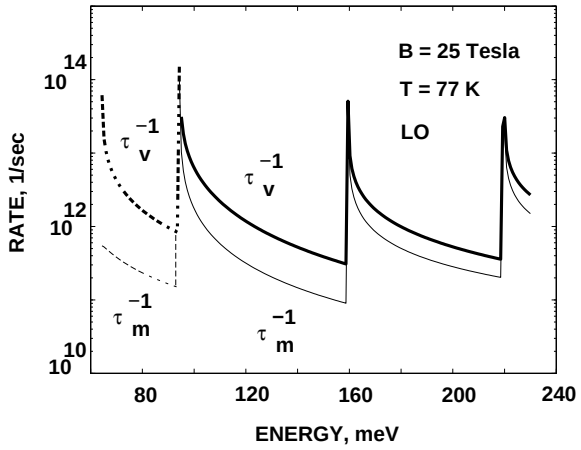

(a)

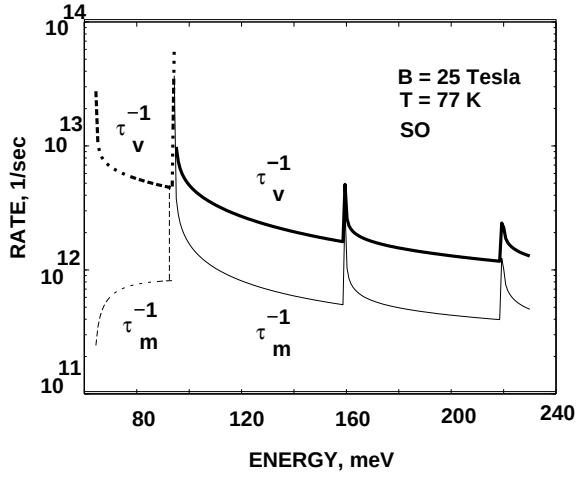

(b)

Figure 4. Velocity and momentum relaxation rates for optical phonon scattering in a magnetic flux density of 25 T at a temperature $T = 77$ K. (a) Confined polar optical phonons (LO), $\hbar\omega_L = 30.2$ meV; (b) surface optical phonons (SO), $\hbar\omega_{SO} = 30.0$ meV.

The allowed scattering mechanisms are then backward and forward absorption only. Backward absorption events that cause a change of the sign in the electron's momentum (type 3 in the inset of figure 3(b)) are suppressed in a strong magnetic field [10]. Thus, the dominant scattering mechanism is forward absorption which causes both velocity and momentum relaxation rates to be negative. This is what we see in figure 4(a).

Once the electron's kinetic energy exceeds the POP energy threshold, intra-subband emission starts to dominate over absorption due to the much higher density of final states (electrons are now scattered to the subband bottom where the density of states is singular). Furthermore, spontaneous emission is much stronger than either absorption or stimulated emission since the Bose distribution factor $N_{\bar{h}\omega_L} \approx 1/147$. However, unlike absorption, intra-subband emission can only cause a loss of momentum and velocity with or without a change in the sign of the wavevector (transitions of type 1 and 2 in the inset of figure 3(b)). Type 1 scattering is quenched in a magnetic field, but events of type 2 are not. Thus, at electron energies past the POP threshold, the onset of intra-subband emission reverts the signs of both velocity and momentum relaxation rates to positive. Again, this is what we observe in figure 4(a).

Inter-subband absorption and emission (whose thresholds correspond to the third and fourth peaks in figure 4(a)) are similar to intra-subband emission in the sense that they too can only cause a loss of momentum with or without a change of the wavevector's sign. Therefore, these two types of scattering mechanism also lead to a positive sign of the velocity and momentum relaxation rates. Consequently, we see only positive relaxation rates at energies larger than the POP threshold (or past the second peak) in figure 4(a). The situation would have been more complicated had a phonon energy been much larger than the energy of subband separation. In that case, inter-subband absorption could conceivably take an electron very high up in the destination subband and increase its velocity causing a negative velocity relaxation rate while maintaining a positive momentum relaxation rate. This is somewhat akin to the transition of the type A–D shown in figure 1. This process requires rather wide wires and materials with large effective mass so that the subband separation in energy is smaller than the phonon energy. We do not meet this requirement with our InAs wire of cross-section 500 Å $\times$ 40 Å, so this process is absent.

Figure 4(b) shows the momentum and velocity relaxation rates for surface optical phonon scattering. The surface optical phonon energy was calculated for a free-standing quantum wire following the prescription in [11, 13]. For an InAs wire surrounded by vacuum ($\epsilon_\infty = 1$), $\bar{h}\omega_{SO} = 30.0$ meV. The rates exhibit the same features as in figure 4(a) and the only additional feature is that the difference between τ_v^{-1} and τ_m^{-1} is larger at high energies. This particular scattering mechanism is very anisotropic at high energies and 'prefers' interactions with phonons of small wavevectors. The associated transitions are almost vertical (see type '2' in figure 2). Consequently, they are not effective in relaxing momentum, but more efficient in relaxing velocity. This leads to a more pronounced difference between τ_v^{-1} and τ_m^{-1}.

Finally, in figure 5, we show the total momentum and velocity relaxation rates obtained by summing over the acoustic phonon, POP and SO phonon rates. Impurity and interface scattering are neglected since their rates are three orders of magnitude smaller than the phonon rates even in relatively dirty wires. The total rates mirror the acoustic phonon scattering rates since those are, by far, the largest. This is a fortuitous turn of events since only the acoustic phonon rates exhibit *opposite signs* over finite energy regions in our chosen example. It is also true that confinement of acoustic phonons is important since it is confinement that increases the scattering rates by three to four orders of magnitude over bulk acoustic phonon scattering rates [13] thus making it the dominant scattering mechanism. The energy windows within which τ_v^{-1} and τ_m^{-1} have opposite signs are actually quite wide (several tens of meV). This allows ample space to place the electron distribution within the window and thus produce

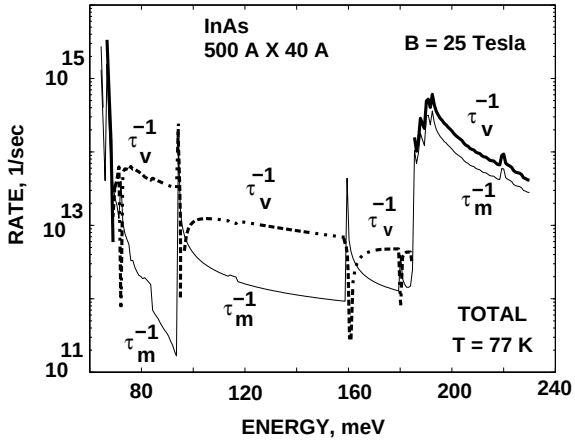

Figure 5. Overall velocity and momentum relaxation rates in a magnetic flux density 25 T and at a temperature $T = 77$ K. All phonon scattering mechanisms are included.

ensemble-averaged rates that have opposite signs. We stress that the width of the window is larger for materials with low effective mass and wires of small cross-section. These two properties are thus conducive to producing momentum and velocity relaxation rates of opposite signs.

3. Ensemble-averaged rates

We now proceed to calculate *ensemble-averaged* momentum and velocity relaxation rates by averaging over the electron distribution function $f_\nu(v_k)$ in every magnetoelectric subband [3]:

$$\left\langle \frac{1}{\tau_m} \right\rangle = \left(\sum_{k,\nu} f_\nu(v_k) k \frac{1}{\tau_m^\nu(k)} \right) \Big/ \left(\sum_{k,\nu} f_\nu(v_k) k \right) \tag{3}$$

$$\left\langle \frac{1}{\tau_v} \right\rangle = \left(\sum_{k,\nu} f_\nu(v_k) v_k \frac{1}{\tau_v^\nu(k)} \right) \Big/ \left(\sum_{k,\nu} f_\nu(v_k) v_k \right). \tag{4}$$

We assumed that only the lowest magnetoelectric subband is occupied ($\nu = 1$) and that the distribution function is a drifted Maxwellian given by $f(v) = \exp(-m^*(v - v_d)^2/2kT_e)$, where T_e is the electron temperature and v_d the drift velocity. Since in all of our calculations kT_e is more than an order of magnitude smaller than the subband separation, the occupation of only one subband is a justifiable assumption. Furthermore, it is well known that the drifted Maxwellian is an excellent approximation in the limit of strong electron–electron scattering. We will assume that electron–electron scattering is frequent; yet we do not need to include this process in the calculation of the total rate since electron–electron scattering does not contribute to *ensemble-averaged* momentum or velocity relaxation. In this type of scattering, whatever momentum or velocity one electron loses is picked up by the other electron (we will neglect Umklapp and anything other than binary electron–electron collisions), so the ensemble as a whole does not gain or lose momentum from electron–electron collisions. These collisions can however affect the ensemble-averaged relaxation rates indirectly by altering the shape of the distribution function. This is a weak second-order effect [14] and, in any case, this is already taken into account when we assume a drifted Maxwellian shape for the distribution.

For convenience, we will convert the summation over the wavevector in equations (3) and (4) to an integration over energy according to the following procedure:

$$\begin{aligned}\sum_k f(v_k)k\frac{1}{\tau_m(k)} &= \sum_{k>0} f(v_k)k\frac{1}{\tau_m(k)} + \sum_{k>0} f(v_{-k})(-k)\frac{1}{\tau_m(-k)} \\ &= \sum_{k>0} f(v_k)k\frac{1}{\tau_m(k)} - \sum_{k>0} f(-v_k)k\frac{1}{\tau_m(k)} \\ &= \sum_{k>0}[f(v_k) - f(-v_k)]\,k\frac{1}{\tau_m(k)} = \frac{L}{2\pi}\int \mathrm{d}k\ [f(v_k) - f(-v_k)]\,k\frac{1}{\tau_m(k)} \\ &= \int \mathrm{d}E\ D(E)\,[f(v_E) - f(-v_E)]\,k(E)\frac{1}{\tau_m(E)} \qquad (5)\end{aligned}$$

where $k(E)$ and $v(E)$ are absolute values of electron wavevector and velocity at an energy E and $D(E)$ is the electron density of states which is found from a numerical solution of the Schrödinger equation in a magnetic field as outlined in reference [5]. The same procedure is applied to all other summations in equations (3) and (4).

3.1. Conditions conducive to the observation of negative velocity relaxation rates and positive momentum relaxation rates for an electron ensemble

It is obvious from equation (5) that if we wish to realize a situation where the ensemble-averaged momentum and velocity relaxation rates will have opposite signs, we will need to centre the distribution function within the energy window where the signs are opposite. To facilitate this process, we will need a narrow distribution and a wide window. A very low lattice temperature (we will assume that the electron temperature $\geqslant$ the lattice temperature) makes the distribution function narrow, but it also makes the window narrower because it inhibits acoustic phonon (forward) absorption which is the main cause for the velocity relaxation rate

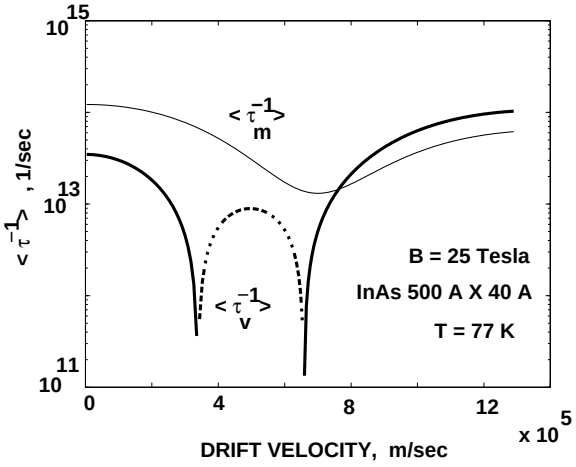

Figure 6. Ensemble momentum and velocity relaxation rates obtained by averaging over a drifted Maxwellian distribution function. The rates are plotted versus the drift velocity. The thin and thick curves indicate momentum and velocity relaxation rates respectively. A broken curve indicates a negative rate and a solid curve a positive rate. The electron and lattice temperatures $T_e = T = 77$ K. There is a window in the drift velocity (3.5×10^7–6.5×10^7 cm s^{-1}) within which the ensemble velocity relaxation rate is negative, but the ensemble momentum relaxation rate is positive.

to be negative. Thus, arbitrary reduction of temperature does not help and there is an optimum temperature. On the other hand, a low effective mass and a narrow cross-section of the wire always help since they increase the energy separation between subbands and widen the window. In fact, we did not find a negative ensemble-averaged velocity relaxation rate in GaAs wires of reasonable cross-section and at reasonable magnetic fields (irrespective of the parameters of the distribution function, namely the lattice temperature and the drift velocity), but found it in InAs wires because of the much lower effective mass.

In figure 6, we show the calculated momentum and velocity relaxation rates averaged over an electron ensemble described by a drifted Maxwellian with temperature $T_e = T_{lattice} = 77$ K as functions of ensemble drift velocity v_d. There is a range of drift velocity between 3.5×10^7 and 6.5×10^7 cm s^{-1} where the velocity relaxation rate is negative, but the momentum relaxation rate is positive. The minimum drift velocity in this window is lower than the peak drift velocity (4.2×10^7 cm s^{-1}) in bulk InAs [15], so it should be possible to observe this effect in real situations.

4. Conclusions

In conclusion, we have shown that it is possible for an electron ensemble in a quantum wire to have simultaneously a negative average velocity relaxation rate and yet a positive average momentum relaxation rate when a magnetic field is present. Thus, the ensemble as a whole gains velocity by colliding with the lattice but loses momentum. In the past, an ensemble-averaged negative momentum relaxation rate was predicted in at least two contexts both of which pertain to quantum wire structures. The first was associated with a dominance of polar optical phonon forward absorption below the optical phonon emission threshold [16] and the second arose from a preponderance of forward acoustic phonon absorption below the acoustic phonon emission threshold [17]. Neither of these two effects required a magnetic field. We point out that the effect discussed in this paper is different and requires a magnetic field. The present effect leads to opposite signs of the ensemble-averaged momentum and velocity relaxation rates which is, in some sense, more intriguing than either of the two rates becoming negative individually. The negative ensemble-averaged velocity relaxation rate does not lead to a negative absolute mobility [17]; instead, it precludes a stable velocity distribution. If the ensemble drifts into the window where the rate is negative, the velocity will continue to increase with time until the ensemble moves out of the window. Thereupon, a stable, steady-state velocity distribution will be established with a positive ensemble-averaged relaxation rate. Thus, the experimental manifestation of a negative velocity relaxation rate is simply a pronounced (transient) velocity overshoot effect which can be enhanced (and controlled) by an external magnetic field.

Acknowledgment

This work was supported by the US Army Research Office under a Short Term Analytical Service agreement.

References

[1] Jackson J D 1962 *Classical Electrodynamics* (New York: Wiley) p 408
[2] Feynman R P, Leighton R B and Sands M 1965 *The Feynman Lectures on Physics* vol III (Reading, MA: Addison-Wesley) p 21–5

[3] Lundstrom M S 1990 *Fundamentals of Carrier Transport (Modular Series on Solid State Devices vol 10)* (Reading, MA: Addison-Wesley)
[4] A detailed examination of the matrix element for scattering shows that it is the dynamical (crystal) momentum $\hbar k$, and not necessarily the kinematic momentum, that is conserved in a scattering process, i.e. $k' = k \pm \gamma$.
[5] Chaudhuri S and Bandyopadhyay S 1992 *J. Appl. Phys.* **71** 3027
[6] Beenakker C W J and van Houten H 1991 *Solid State Physics* vol 44, ed H Ehrenreich and D Turnbull (San Diego, CA: Academic) p 99
[7] Free-standing wires are now routinely fabricated by impregnating naturally occurring 30 nm diameter pores (or nanotubes) in matrices such as crysotile asbestos with the semiconductor of choice. See, for instance, Poborchi V V, Ivanova M S and Salamatina I A 1994 *Superlatt. Microstruct.* **16** 133
[8] Svizhenko A, Bandyopadhyay S and Stroscio M A 1998 *J. Phys.: Condens. Matter* **10** 6091
[9] Svizhenko A, Balandin A, Bandyopadhyay S and Stroscio M A 1998 *Phys. Rev.* B **57** 4687
[10] Telang N and Bandyopadhyay S 1993 *Appl. Phys. Lett.* **62** 3161
[11] Mori N and Ando T 1989 *Phys. Rev.* B **40** 6175
[12] Adachi S 1992 *Physical Properties of III–V Compound Semiconductors: InP, InAs, GaAs, GaP, InGaAs and InGaAsP* (New York: Wiley)
[13] Kim K W, Stroscio M A, Bhatt A, Mickevicius R and Mitin V V 1991 *J. Appl. Phys.* **70** 319
[14] Ziman J M 1960 *Electrons and Phonons* (Oxford: Oxford University Press)
[15] Dobrovolskis Z, Grigoras K and Krotkus A 1989 *Appl. Phys.* A **48** 245
[16] Riddoch F A and Ridley B K 1984 *Surf. Sci.* **142** 260
[17] Telang N and Bandyopadhyay S 1994 *Phys. Rev. Lett.* **37** 1683